sciendo

*Polish Journal of Chemical Technology, 25, 1, 47—60, 10.2478/pjct-2023-0008*

# Green method of conversion of geraniol to value-added products in the presence of selected minerals

**Anna Fajdek-Bieda[1], Agnieszka Wróblewska[2*], Andrzej Perec[1], Piotr Miądlicki[2]**

*[1]Jacob of Paradies University, Faculty of Technology, Chopina 52, Gorzow Wielkopolski, 66-400, Poland*
*[2]West Pomeranian University of Technology, Szczecin, Faculty of Chemical Technology and Engineering, Department of Catalytic and Sorbent Materials Engineering, Pułaskiego 10, Pl 70-322 Szczecin*
*[*]Corresponding author: e-mail: agnieszka.wroblewska@zut.edu.pl*

The study presents the results of research on the process of geraniol (GA) transformation in the presence of natural minerals: montmorillonite, mironekuton, halloysite and also in the presence of halloysite modified with 0.1 M water solution of $H_2SO_4$. To obtain information on the structure of the used catalysts, instrumental studies were performed (SEM, XRD, FT-IR, XRF, BET). The second part of the research consisted in examining the influence of individual parameters (temperature, catalyst content, and reaction time) on the course of GA transformation process. The syntheses were carried out without the application of solvent and under atmospheric pressure. To determine the most beneficial process conditions, two functions were selected: GA conversion and selectivity of GA. The proposed method of GA transformation on such minerals: montmorillonite, mironekuton, halloysite, has not been described in the literature so far.

**Keywords:** halloysite, mironekuton, geraniol, linalool, thumbergol.

## INTRODUCTION

The process of isomerization of compounds of natural origin is important for many industrial sectors. The resulting compounds are valuable intermediates in perfumery, cosmetics, medicine and even in mechanical engineering. Catalytic processes running with the participation of catalysts showing high activity play today also an important role, because the use of such catalysts increases the conversion of the raw material and also it often causes an increase in the selectivity of the transformation of organic raw material to the main product of the process[1, 2].

Geraniol (GA, unsaturated terpene alcohol) found in many essential oils, including lemon, ginger and lime, has an intense aroma with a hint of freshness. Natural geraniol is obtained mainly from pelargonium, and it is applicable in many fragrance compositions. Moein and Eng.[3] examined the chemical composition of 10 samples of rose water. The essential oils have been extracted and identified using the GC/MS method. Phenethyl alcohol, geraniol and β-citronellol was the main ingredient in most of the samples. Geraniol was present in large amounts in half of the samples (1–11.67%, 2–3.95%, 3–2.34%, 4–24.01%, 5–12.59%).

GA shows the strongest bactericidal activity, mainly against *Escherichia coli* and *Salmonella enterica*. Moreover, geraniol helps to inhibit the development of prostate, liver, skin and intestine cancer cells. Additionally, geraniol is a compound that can undergo numerous transformations (Fig. 1, Scheme 1) into valuable compounds used in the industrial production of fragrances, perfumes, aromas, and therapeutic agents[4].

The transformation of GA was the subject of studies in several research centers. Yu et al.[12] presented the process of transformation of the GA in which $FeCl_2 \times 6H_2O$ was used as a catalyst. The main products obtained in this process were linalool and α-terpineol. The process was carried out in the presence of acetonitrile as a solvent, to which GA was first added and then the catalyst. The synthesis was carried out for 4 hours at room temperature. Haese et al. in their publication[13] presented studies of the GA transformation process for geraniol in a pure form and geraniol in a mixture with nerol. It turned out that the results obtained for pure geraniol are the same as for geraniol mixture with nerol. Other scientists presented the transformation of geraniol under the influence of gamma radiation. The process involved irradiating of GA-methanol solution to obtain nerol and linalool. The maximum value of the geraniol conversion was 30%.

Other studies were carried out with the use of micro--and micro-mesoporous BEA-type zeolites. The syntheses were carried out in the temperature range from 27 to 150 °C for 1-2 hours. It was a solvent-free process, carried out under nitrogen and argon atmosphere. It turned out that GA was converted to linalool and nerol, as well as to (2E, 6E) -6,11-dimethyl-2,6,10-dodecatriene-1-ol and (trans, trans-farnesol – (2E), 6E)) -3,7,11-trimethyl--2,6,10-dodecatrien-1-ol). The conversion obtained for GA was 99%[14].

In the work of Tsitsishvili et al.[15], the catalytic transformations of terpene alcohols (geraniol) were used in the perfume industry on micro- and micro-mesoporous zeolites of the BEA type. Experiments were performed using various catalyst/geraniol mass ratios (0.0075–0.053 g/g), in an inert atmosphere (nitrogen, argon) and at a temperature of 27 to 150 °C. The analysis of catalytic transformation products was performed by gas chromatography – mass spectrometry (GC-MS). Geraniol conversion, product yield and selectivity were calculated based on experimental data. The reaction products mainly contained unreacted trans-geraniol, β-linalool, trans,trans--farnesol and (2E, 6E)-6,11-dimethyl-2,6,10-dodecatrien--1-ol, and small amounts of β-myrcene, D-limonene, trans-β-ocimene, β-ocimene, α-terpineol, cis-geraniol, cis-isogeraniol, trans, trans, trans-geranylgeraniol, p- and m-camphor. It turned out that the method with the application so-called "zeolite reactor" can be obtained such long chain molecules like trans, trans-farnesol and (2E, 6E)-6,11-dimethyl-2,6,10-dodecatrien-1-ol in relatively low temperature and with increased selectivity to 37

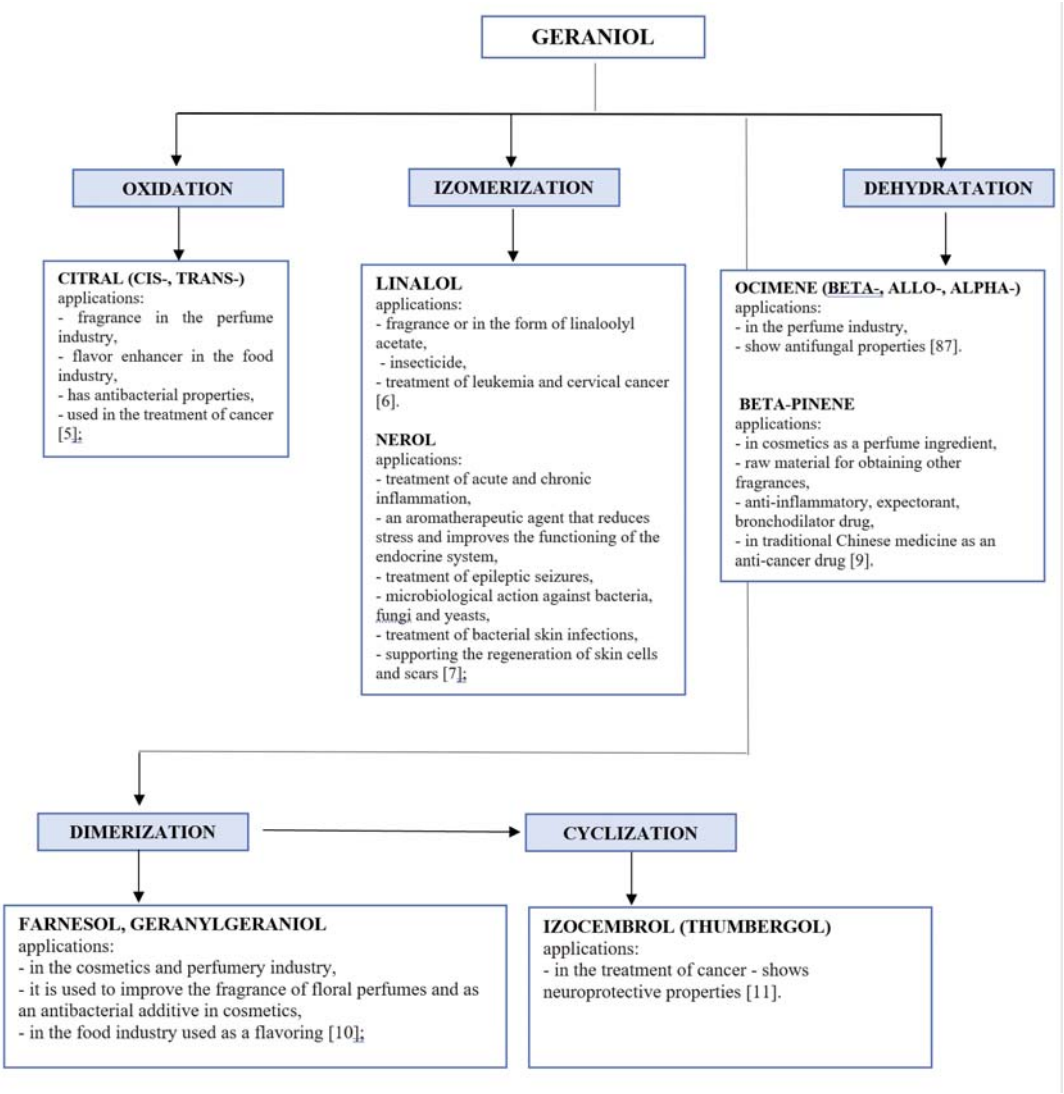


**Figure 1.** Diagram of the main reactions taking place during the transformation of geraniol and a description of the applications of the main products

and 52%, respectively. In addition, trans,trans-farnesol attaches one more isoprene unit to the mold long chain trans, trans, trans-geranylgeraniol molecule that can form a macrocycle thunbergol $C_{20}H_{34}O$.

Fajdek-Bieda et al. studied the GA transformation process with the use of two natural zeolites: sepiolite[16] and clinoptilolite[17]. The tests assessed the influence of the following parameters: temperature (in the range from 80 to 150 °C), catalyst content (in the range from 5 to 15 wt%) as well as reaction time (in the range from 15 to 1440 minutes). As a result of the process carried out in the presence of sepiolite, the following products were obtained: β-pinene (BP), ocimenes (OC), linalool (LO), nerol (NE), citral (CL), isocembrol (IC) and thumbergol (TH). The highest selectivity (19 mol%) was obtained for LO. When clinoptilolite was used, the main products were 6,11-dimethyl-2,6,10-dodecatrien-1-ol (DC) and thumbergol (TH). The highest values of the selectivity of DC (14 mol%) and TH (47 mol%) were obtained at the temperature of 140 °C for the catalyst content 12.5 wt% and for the reaction time of 180 min.

Aluminosilicates are popular porous materials that are very often used in catalytic processes[18–20]. An example of aluminosilicate is halloysite (HAL) which contains approx. 45% silica and approx. 40% alumina. The other ingredients are mainly water and traces of metal oxides, ie. $Al_2O_3$, FeO, MgO, $K_2O$, CaO, $Na_2O$, and $TiO_2$. HAL has very small, cylindrical crystals. In addition, it contains admixtures of chromium, iron, magnesium, nickel and copper. At the temperature of about 60 °C and with longer drying, it begins to lose water, which results in its transformation into metahalloysite - with a chemical composition identical to kaolinite, but with a different, disturbed structure[21–26]. HAL present in Polish deposits is characterized by a specific plate-like structure, with a predominance of the plate fraction. Due to the specific layer-and-tube structure, halloysite can be transformed into an active material that is used in many industries and environmental protection[27–29]. HAL has been used as a sorption agent in the production of insulating mats[30], fertilizers, feed additives[31], cosmetic clays[32], coagulants[33], pigments for paints and biofilters[34–36].

Montomrillonite (MMT) is an aluminosilicate, with a structure consisting of three 2 : 1 layers. Two of them are tetrahedral sublayers and one is octahedral sublayer, which are connected by van der Waals forces. Additionally, the space between the layers is filled with both water and metal cations, including $Li^+$, $Na^+$, $Mg^{2+}$, $Ca^{2+}$ and $Al^{3+}$. As a result of ion exchange, metal cations can be substituted with other metal cations, thereby affecting the properties of MMT. Moreover, the hydrophilic nature of MMT makes it easily susceptible to modification

with both organic and inorganic compounds[37–38]. MMT is one of the most extensively studied minerals in the field of heterogeneous catalysis. This is mainly due to its unique properties, such as very good cation exchange and adsorption ability[39].

Mironekuton (MIR) is a sedimentary rock found in only one region of Japan, on the island of Honshu. MIR particles are very porous and have micropores with a diameter of only 50 nm. These mesopores cause that MIR has remarkable adsorption properties. MIR mainly consists of $SiO_2$ (55 wt%), $Al_2O_3$ (13 wt%), CaO (3.6 wt%), MgO (1.6 wt%), sulfur, potassium and oxides, among others titanium, phosphorus, cobalt, sodium or manganese. MIR is used in shrimp breeding because it creates the right conditions for the development of bacteria in water that support the growth of plants that produce shrimps. In addition, it stabilizes pH of water, absorbs harmful substances and odors, and accelerates the photosynthesis process[40].

The minerals described above, due to their unique properties, have found applications in chemical processes. Halloysite, as a natural material with a nanotube structure, has found a number of technological applications, as a mineral adsorbent (adsorbs toxic substances and heavy metals), a catalyst carrier, a modifier for rigid polyurethane-polyisocyanurate (PUR-PIR) foams, a filler for the modification of polypropylene (PP) and for reducing the concentration of pollutants in municipal wastewater[41, 42]. Metal-modified montmorillonite plays a key role in the oxidation of toxic organic pollutants, such as phenol, substituted phenols and dyes, in aqueous solutions under mild conditions. This mineral has found application in the hydrogenation of nitrobenzene to aniline as well as in the 1,3-dipolar cycloaddition between terminal alkynes and azides to obtain highly regioselective 1,4-unsubstituted mono- and bis-1,2,3-triazoles[43]. In the case of mironekuton, the use of this mineral in chemical processes has not been described so far.

This work aimed to develop the most favorable conditions for the preparation of one (or possibly two) products of geraniol transformation with the use of such catalysts as MMA, MIR and HAL. We also decided to modify the surface of HAL by washing with a 0.1 M sulfuric acid solution, which was to increase the HAL activity (HAL-MOD was obtained). The first part of this work was devoted to instrumental tests (XRD, SEM, FT-IR, XRF) of catalysts used in transformations of geraniol. The obtained results made it possible fully characterize their physicochemical properties. The second part of the work concerns the research on the influence of temperature, catalyst content and reaction time on the course of the GA transformation process under atmospheric pressure. The presented method has many advantages, such as the use of low reaction temperatures, low catalyst content and optimally short reaction times. In addition, the syntheses are carried out without the presence of the solvent, which eliminates the possibility of its reaction with the GA and its transformation products. Additionally, there is no need to recover and recycle solvent. Moreover, the presented solution which uses HAL, HAL-MOD, MMA and MIR has not been described in the literature so far.

**PRODUCTS OF GERANIOL TRANSFORMATION**

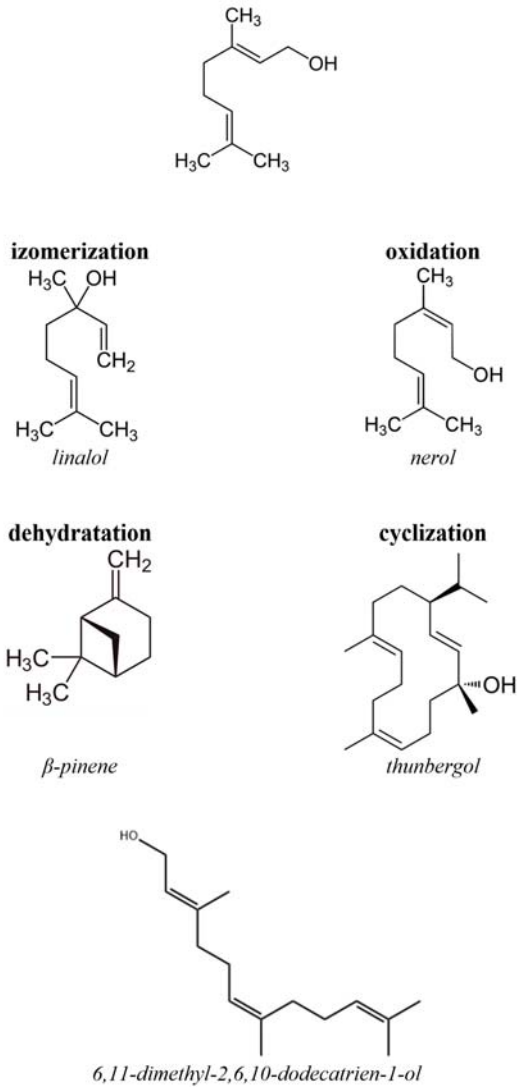


**Scheme 1.** Products of geraniol transformation in the presence of selected minerals

## MATERIALS AND METHODS

### Raw materials

Table 1 presents information on the raw materials used.

**Table 1.** Raw materials

| CHEMICAL COMPOUND | CLEANLINESS | BUSINESS/COUNTRY |
|---|---|---|
| montmorillonite | 100% | Zębiec S.A., Kraków, Poland |
| halloysite | 100% | Dunino, Wrocław, Poland |
| mironekuton | 100% | Newstone International Corporation, Chicago, USA |
| geraniol | 99 % | Acros Organics, Chicago, USA |
| linalool | 97% | |
| farnesol | 96% | |
| nerol | 97% | |
| citronellol | 95% | Sigma Aldrich, Chicago, USA |
| myrcene | technical grade | |
| geranylgeraniol | 85% | |
| citral | 95% | |
| ocimene | 90% | |
| betapinene | 95% | |

**Table 2.** Instrumental tests of the catalysts

| Method | | Business/Country |
|---|---|---|
| X-ray difraction (XRD) | Empyrean X-ray difractometer with a Cu Kα radiation source; Samples were analyzed in the temperature 5–30° with step size of 0.02°; | Malvern Panalytical, London, UK |
| Specifc surface area (SSA), total pore volume (TPV) and micropore volume (MV) | Measurement by nitrogen adsorption at 350 °C using the QUADRASORB evoTM Gas Sorption Surface and Pore Size Analyzer; The sample was degassed at 250 °C for 20 h under N2; | Quantachrome Instruments, Chicago, USA |
| Element mapping by scanning electron microscopy (SEM) and corresponding EDX spectrum of surface | made with ultra-high resolution SEM field emission, secondary electron detector was used Elemental analysis was performed using an Epsilon3 spectrometer with X-ray energy dispersion; | JEOL, JSM-6010LA, Malvern Panalytical,London, UK |
| Infrared spectroscopy (FT-IR) | analysis carried out in the range of wavenumbers from 400 to 4000 $cm^{-1}$; | Thermo Nicolet 380 apparatus, Berlin, Germany |

### Instrumental studies of catalysts

The following instrumental studies were performed for each of the catalysts (Table 2).

### Method of transformations of geraniol

The syntheses connected with geraniol transformations in the presence of the tested catalysts were carried out in a glass reactor with a capacity of 25 $cm^3$, equipped with a reflux condenser and a magnetic stirrer with heating function (Fig. 2). The tested parameters were changed in the following ranges: temperature 80–150 °C, catalyst content 5–15 wt%, and reaction time from 15 minutes to 24 h.

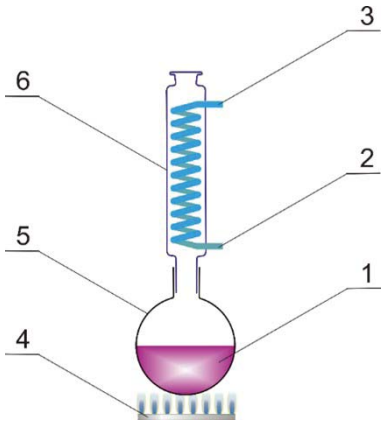


**Figure 2.** Scheme of the apparatus for carrying out the syntheses connected with the transformations of geraniol: 1 – reaction mixture, 2 – water outlet, 3 – water inlet, 4 – heating, 5 – round bottom flask, and 6 – reflux condenser

### Analyses of the post-reaction mixtures

To perform a qualitative and quantitative analysis, the reaction mixture had to be centrifuged and dissolved in acetone in a weight ratio of 1:3. Qualitative analyzes were performed using the GC-MS method using the Thermo-Quest apparatus, which was equipped with a Voyager detector and a DB-5 column with a phenylmethylsiloxane packing (30 m x 0.25 mm x 0.5 mm). Analysis parameters were as follows: helium flow 1 ml/min, sample chamber temperature 200 °C, detector temperature 250 °C, furnace temperature - isothermal for 2.5 minutes at 50 °C, then heating at the rate of 10 °C/ min to 300 °C.

The quantitative analyses of the obtained products were performed using a Thermo Electron FOCUS chromatograph equipped with an FID detector and a TR-FAME column packed with cyanopropylphenyl (30 m x 0.25 mm x 0.25 mm).

The FID was kept at 250 °C. Two methods were used to quantify the reaction products in the reaction mixture:

– external standard method using commercially available chemical standards – 8-point calibration curves were made for each compound in the concentration range of 0.33 wt.%,

– an internal standardization method.

Mass balances for the syntheses made it possible to calculate the geraniol conversion ($C_{geraniol}$) and the selectivity formation of the various products ($S_{product/geraniol}$).

$$\mathbf{S_{product/geraniol}} = \frac{\mathrm{AMP}}{\mathrm{AMGC}} \cdot 100\% \quad (1)$$

where: AMP – the amount of moles of product, AMGC – the amount of moles of geraniol consumed,

$$\mathbf{C_{geraniol}} = \frac{\mathrm{AMGC}}{\mathrm{AMGIR}} \cdot 100\% \quad (2)$$

where: AMGC – the amount of moles of geraniol consumed, AMGIR – the amount of moles of geraniol introduced into reactor.

## RESULTS AND DISCUSSIONS

### Morphology of natural catalysts (MMT, MIR, HAL, HAL-MOD)

Figure 3 shows the SEM images for all tested catalysts. Montmorillonite (MMT) consists of particles of irregular shape, 1–10 $\mu$m (Fig. 3a), which form compact and heterogeneous aggregates with smaller grains[44]. The structure of mironecuton (MIR) is shown in Figure 3b. Since the mineral was formed mainly by marine organisms, fossilized remains of ancient crustaceans can be seen in the picture. The above observations have also been confirmed by other authors involved in MIR structure analysis[45]. SEM images for halloysite – HAL (Fig. 3c) and its modified structure – HAL MOD (Fig. 3d) are very similar. They are characterized by different particle shapes, as well as heterogeneity. Treatment of HAL with 0.1M aqueous solution of sulfuric acid did not significantly affect the structure of the mineral[46]. These observations have also been described by other authors[47].

Figure 4 shows the diffraction spectra for MMT, MIR, HAL and HAL-MOD. The obtained diffractograms for all minerals are consistent with those described in the literature[48–53]. MMT shows characteristic diffraction peaks 2θ = 21.4, 2θ = 26.2, which are characteristic of its structure (JCPDS card 29-1498). In the MIR spectrum, a characteristic peak at 2 Theta 2θ = 27.2 can be observed for this mineral. For both HAL and HAL-MOD, characteristic peaks are seen at 2 Theta angles 2θ = 20.2, 2θ = 26.7, 2θ = 35.0 (JCPDS card 29-1489). The diffractograms of HAL and HAL-MOD have a similar

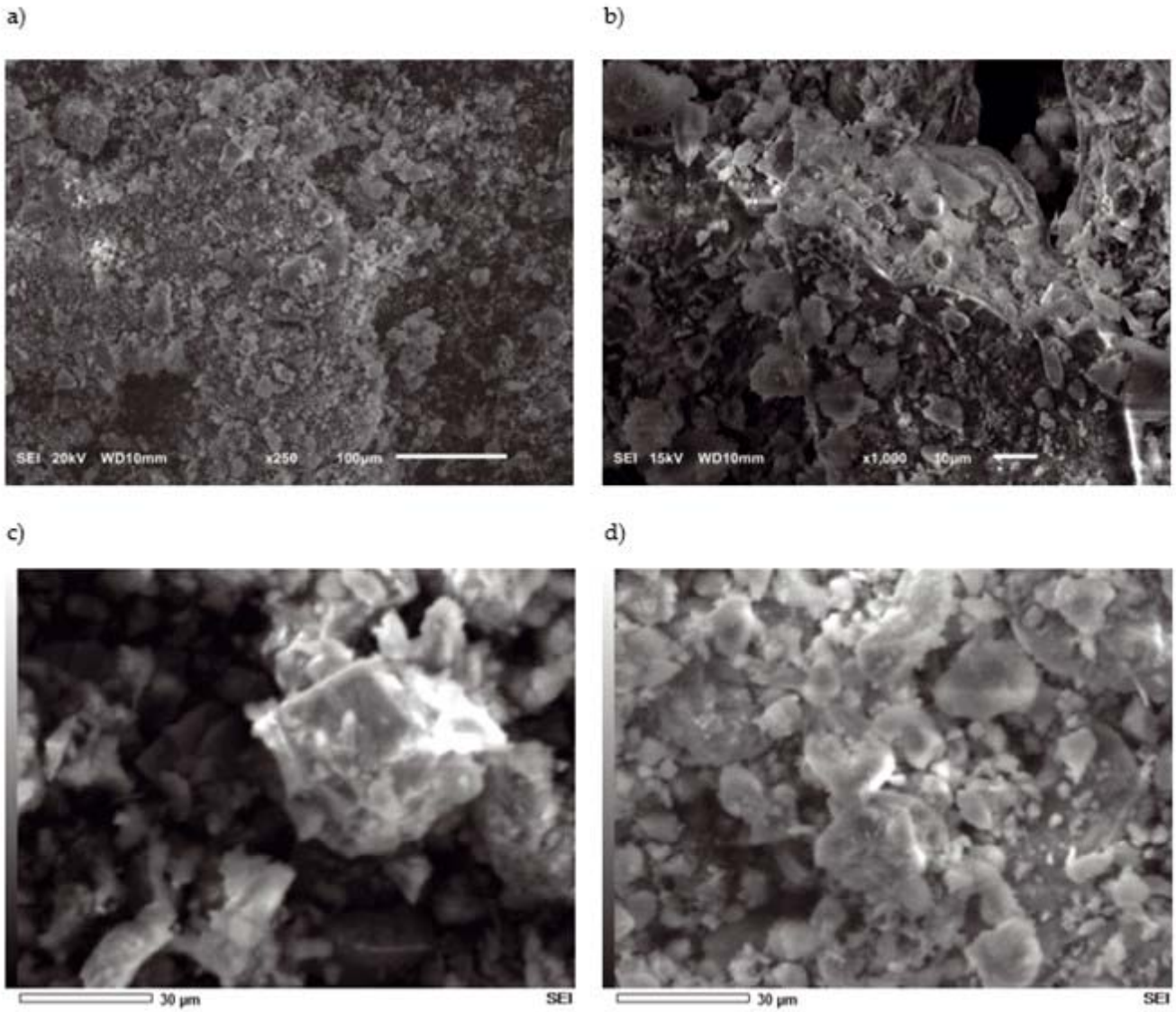


**Figure 3.** SEM images of montmorillonite (a), mironekuton (b), halloysite (c) and modified halloysite (d) catalysts

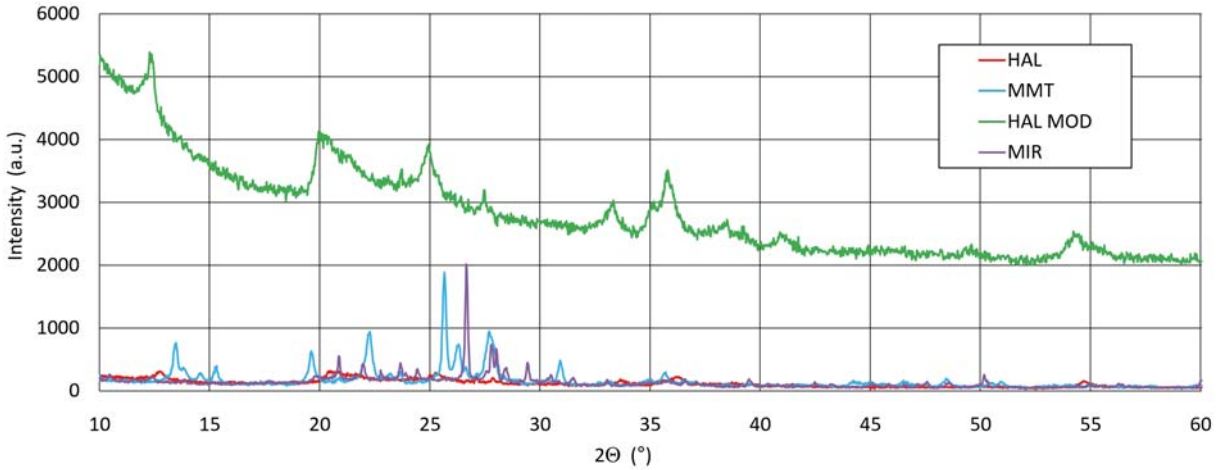


**Figure 4.** X-ray diffraction data for montmorillonite (a), mironekuton (b), halloysite (c) and modified halloysite (d) catalysts

pattern and are consistent with the spectra obtained by other authors[54].

The infrared spectrum for MMT (Fig. 5a) shows the absorption bands at 912 $cm^{-1}$ connected with the Al-O bending vibrations, while bands at 536, 470 and 430 $cm^{-1}$ represent the Al-O-Si skeletal vibrations. Bending vibrations of Si O are represented by bands at 1114–1006 $cm^{-1}$, and tensile vibrations at 796 and 694 $cm^{-1}$. The absorption band at 1627 $cm^{-1}$ represents the OH bending vibration. Bands at 3441 and 3410 $cm^{-1}$ indicate the presence of an outer surface stretching -OH. The spectrum obtained is consistent with the literature data[55].

The FTIR spectrum of the MIR is shown in Figure 5b. The characteristic bands occurring at 3448 $cm^{-1}$ and 1635 $cm^{-1}$ correspond to OH stretching vibrations and bending vibrations of hydroxyl groups from water

molecules. The band at 1000 $cm^{-1}$ belongs to metal--oxygen vibrations. The presence of the above bands is confirmed by literature reports[45].

The infrared spectra (Fig. 5 c–d) for Hal and HAL--MOD samples show the vibration bands at 3697 and 3620 $cm^{-1}$ which are assigned to two $Al_2OH$ groups (each OH group is connected to two Al atoms). Moreover, there are visible bands at 3670 $cm^{-1}$ and 3651 $cm^{-1}$ which are attributed to the stretching vibrations of the OH group, the band at 1648 $cm^{-1}$ which corresponds to strongly bending vibrations of adsorbed water, the band at 1107 $cm^{-1}$ which is assigned to the presence of the Si-O group, bands at 1030 and 691 $cm^{-1}$ which are responsible for stretching vibrations of the Si-O-Si groups, bands at 940 and 914 $cm^{-1}$ which are caused by deformation of the OH groups on the inner surface, and bands at 794 and 750 $cm^{-1}$ which can be attributed to the translational vibrations of the OH group. The spectra obtained are consistent with the literature data[56].

The specific surface area (BET) was determined using the Brunauer-Emmett-Teller (BET) equation. The volume of micropores (Vmicrop.) was determined by the DFT model, and the total pore volume (Vpor) was calculated from the volume of nitrogen adsorbed at the pressure p/po. The values of these parameters for the tested catalysts are presented in Table 3. MMT has the highest surface area – 403 $m^2/g$, followed by HAL 132 $m^2/g$, HAL-MOD 66 $m^2/g$ and MIR 26 $m^2/g$. Despite the smallest BET surface area, MIR has the largest total pore volume, which is 0.657 $cm^3/g$. For the remaining catalysts, the values of the total pore volume are very similar. The micropore volume values can be represented in the following order: MIR> MMT> HAL> HAL-MOD.

**Table 3.** Properties surfaces of the tested materials

| Catalyst | BET [$m^2/g$] | V por [$cm^3/g$] | V microp. [$cm^3/g$] |
|---|---|---|---|
| MMT | 403 | 0.213 | 0.145 |
| MIR | 26 | 0.657 | 0.859 |
| HAL | 132 | 0.232 | 0.027 |
| HAL-MOD | 66 | 0.192 | 0.002 |

Figure 6 (a–d) shows the maps of the elements contained in the tested samples. In the case of MMT the presence of seven main components (aluminum, copper, iron, potassium, magnesium, oxygen and silicon) was determined. Figure 6b shows the composition of MIR for which the presence of ten elements was identified: aluminum, carbon, calcium, iron, potassium, magnesium, sodium, oxygen, sulfur, and silicon. On the HAL and HAL-MOD surfaces, the presence of five main elements was identified: oxygen, aluminum, silicon, iron and titanium. In all cases, an even distribution of elements on the surfaces of the catalysts is visible.

The results of the elemental analysis for the tested catalysts are summarized in Table 4 and Figure 7 a–d. In the case of MMT, the highest concentration was obtained

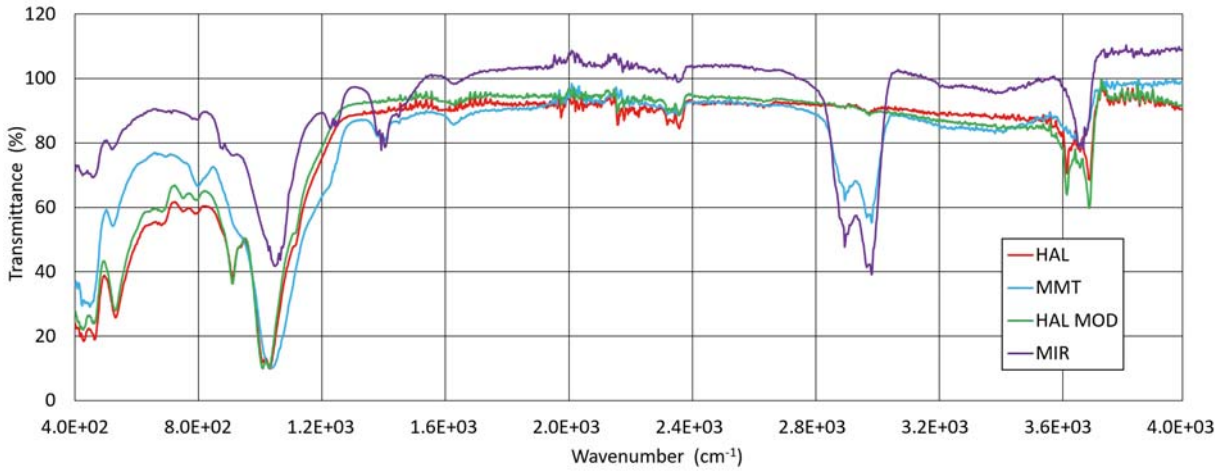


**Figure 5.** The FT-IR spectra of montmorillonite (a), mironekuton (b), halloysite (c) and modified halloysite (d) catalysts

**Table 4.** Results of EDXRF analysis

| Element | | MMT | MIR | HAL | HAL-MOD |
|---|---|---|---|---|---|
| O | Mass % | 49.45 | 46.23 | 40.10 | 48.33 |
| | Atom % | 63.76 | 56.90 | 59.54 | 64.07 |
| Mg | Mass % | 0.89 | 1.15 | – | – |
| | Atom % | 0.76 | 0.93 | – | – |
| Al | Mass % | 6.03 | 6.61 | 16.40 | 18.14 |
| | Atom % | 4.61 | 4.83 | 14.44 | 14.26 |
| Si | Mass % | 39.78 | 27.77 | 17.57 | 23.56 |
| | Atom % | 29.22 | 19.47 | 14.86 | 17.80 |
| K | Mass % | 1.29 | 1.72 | – | – |
| | Atom % | 0.68 | 0.87 | – | – |
| Ti | Mass % | 0.55 | – | 1.35 | 1.95 |
| | Atom % | 0.24 | – | 0.97 | 0.60 |
| Fe | Mass % | 2.01 | 4.44 | 23.97 | 8.61 |
| | Atom % | 0.74 | 1.56 | 10.20 | 3.27 |
| Na | Mass % | – | 0.72 | – | – |
| | Atom % | – | 0.62 | – | – |
| S | Mass % | – | 0.62 | – | – |
| | Atom % | – | 0.38 | – | – |
| Ca | Mass % | – | 2.75 | – | – |
| | Atom % | – | 1.35 | – | – |

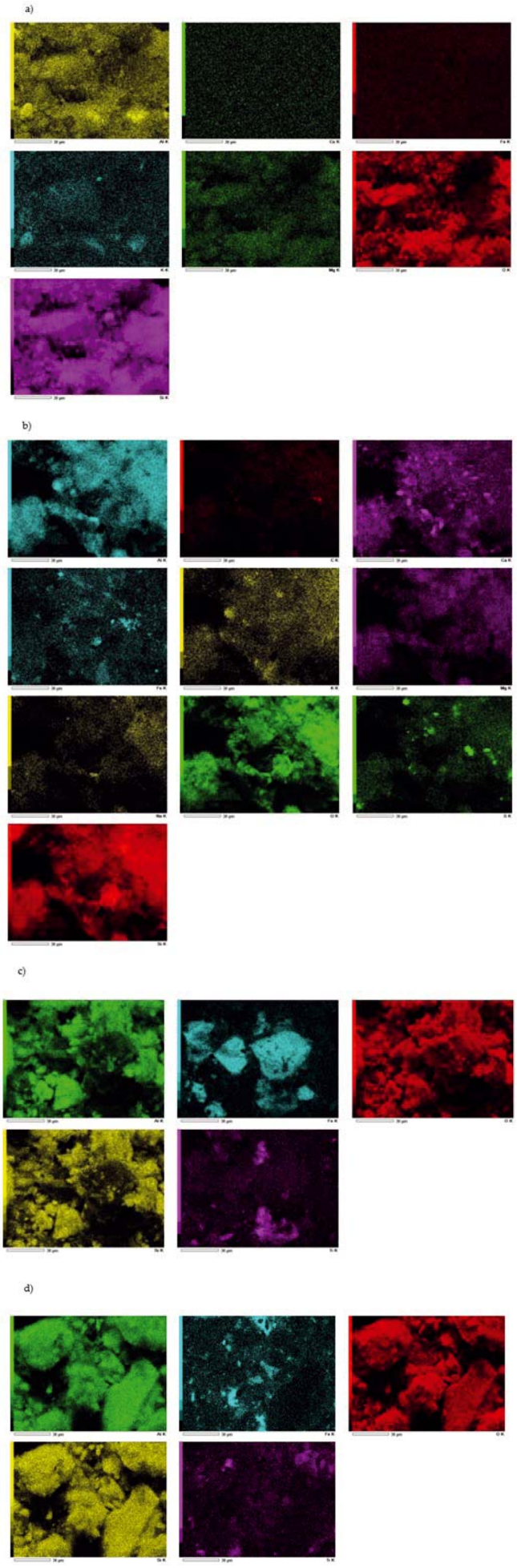


**Figure 6.** Element maps for montmorillonite (a), mironekuton (b), halloysite (c) and modified halloysite (d) catalysts

for O (49.45 mass%), then for Si (39.78 mass%) and Al (6.03 mass%). Moreover, the content of such elements as Mg, K, Ti and Fe was found. In the case of MIR, the same as for MMT, the highest contents were obtained for O, Si and Al. In the structure of this catalyst, the presence of such elements as Mg, K, Fe, Na, S, Ca was also confirmed. The presence of some of them is related to the impurities found in this mineral. In the case of the other two catalysts, HAL and HAL-MOD, an increase in the content of O from 40.10 mass% (HAL) to 48.33 mass% (HAL-MOD) is visible. A similar increase can be seen for elements such as silicon (from 17.57 mass% to 23.56 mass%) and aluminum (from 16.40 mass% to 18.14 mass%). On the other hand, activation with sulfuric acid causes a significant decrease in iron content (HAL 23.92 mass% Fe, HAL-MOD 8.61 mass% Fe), which is related to the decrease in hematite content in the catalyst sample after activation. The obtained results for both catalysts are similar to those obtained by other authors[50, 51, 56].

**The influence of temperature on GA transformation**

As the first parameter, the influence of temperature on the course of the GA transformation process was investigated. The temperature was tested in the range from 50 to 150 °C. The initial parameters were: catalyst content 5 wt% and reaction time 3 h.

Table 5 shows the effect of temperature on the GA conversion function for each of the catalysts tested. When the process is carried out in the presence of MMT, the GA conversion function tends to increase. Initially, it is about 80 mol% at 50 °C, then increases to about 99 mol% at 80 °C. Beyond this temperature, chromatographic analysis showed the presence of only polymerization products (Fig. 8a). With MIR, GA conversion increases from about 63 mol% (80 °C) to about 100 mol% (110 °C). In the higher temperature ranges, the function remains constant, but above 150 °C, only polymerization products are formed, making it difficult to analyze a given synthesis. In the case of HAL, the lowest GA conversion value was obtained at 80 °C, equal to about 53 mol%. When the temperature is increased, the GA conversion value increases to about 99 mol% (in the temperature range from 90 to 150 °C) (Fig. 8b). For HAL-MOD, GA conversion values increase from about 85 mol% (50 °C) to about 99 mol% (80 °C). The acid activation of HAL caused an increase in the content of Ti active sites, resulting in high GA conversion values already at 50 °C. At higher temperatures, a large number of polymerization products are formed, which prevents detailed analysis of the process.

When HAL was used in the process, the main products were DC, TH and NE. The highest values of their selectivity were obtained for TH at about 18 mol% (100 °C), DC 8 mol% (90 °C) and NE 3 mol% (90 °C). Other isomerization products were formed in small amounts

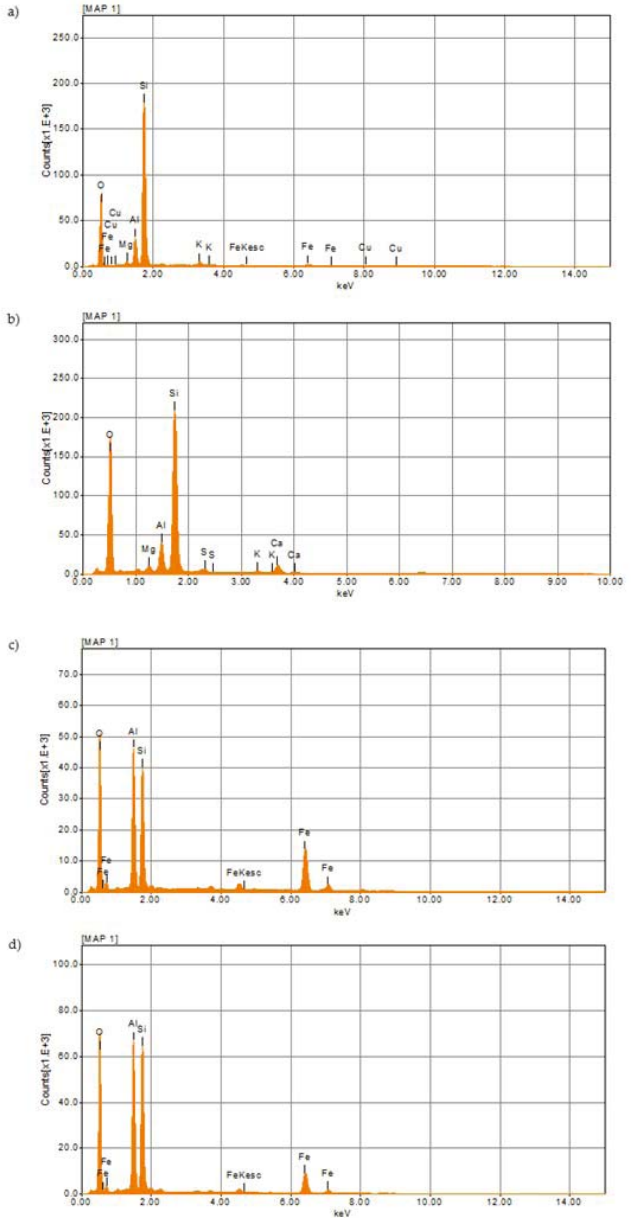


**Figure 7.** The XRF spectra of montmorillonite (a), mironekuton (b), halloysite (c) and modified halloysite (d) catalysts

(Fig. 8c). In the case of HAL-MOD, only one BP product with a selectivity of about 35 mol% is formed in the low temperature range. Only at 80 °C other products formation observed: LO, NE, DC and TH. Above 120 °C, only polymerization products were formed (Fig. 8d). The high activity of HAL-MOD in BP formation can be explained by the effect achieved by modifying the structure of this mineral. Acid activation using inorganic acids (in this case HCl), which in addition to increasing the specific surface area, increases the porosity and adsorption capacity of the mineral and removes impurities. Most likely, BP molecules are formed on the catalyst surface, on which Ti active centers are located. On the surface, the geraniol molecule transforms from

**Table 5.** The influence of temperature on the conversion of GA

| Conversion of GA (mol%) | Temperature (°C) | | | | | | | | | |
|---|---|---|---|---|---|---|---|---|---|---|
| | 50 | 60 | 70 | 80 | 90 | 100 | 110 | 120 | 130 | 140 | 150 |
| MMT | 80.43 | 81.52 | 86.20 | 99.29 | polymerization products | | | | | | |
| MIR | 62.98 | 64.38 | 64.18 | 99.58 | 99.71 | 99.56 | polymerization products | | | | |
| HAL | – | – | – | 52.80 | 99.43 | 99.26 | 98.64 | 98.97 | 98.69 | 98.85 | 98.90 |
| HAL-MOD | 84.60 | 84.39 | 91.98 | 99.13 | polymerization products | | | | | | |

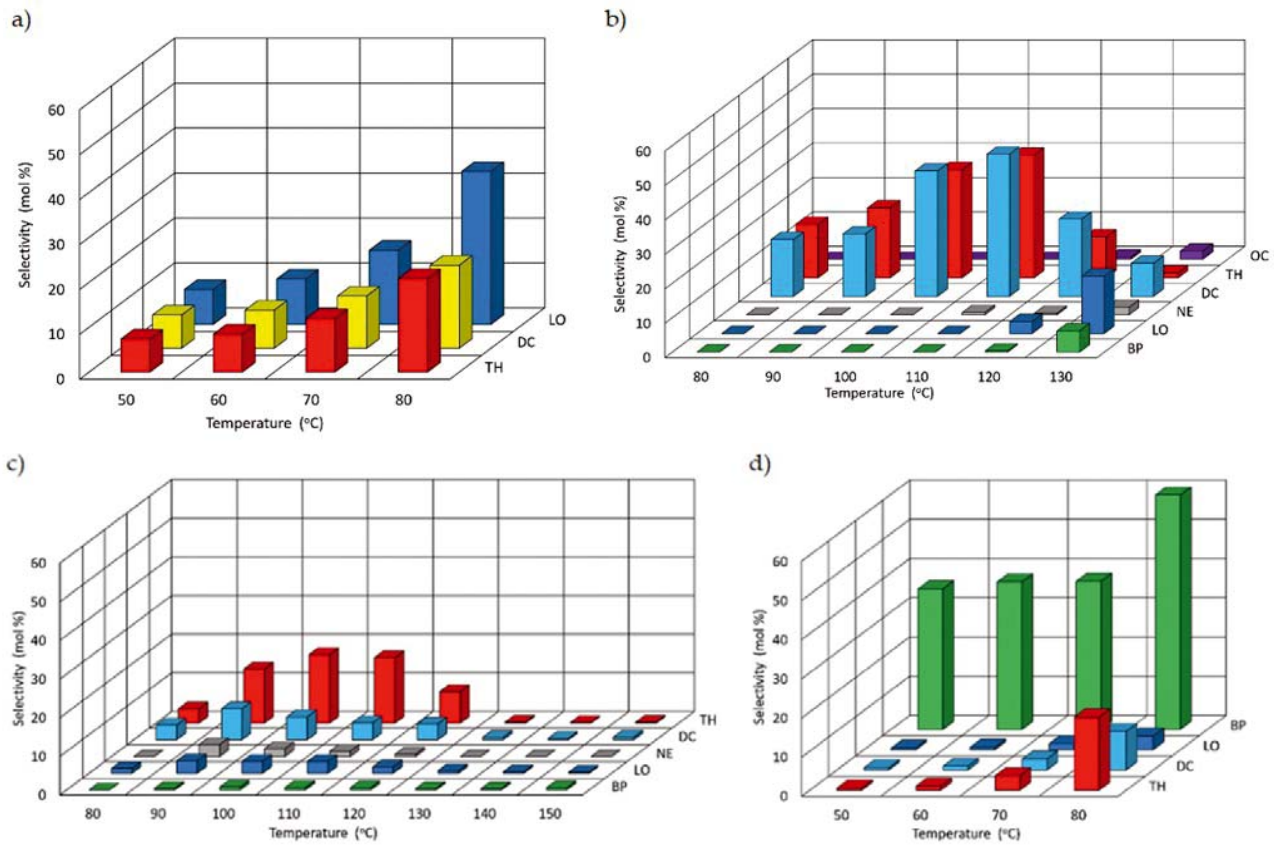


**Figure 8.** The influence of temperature on the selectivities of the appropriate products over (a) MMT, (b) MIR, (c) HAL and (d) HAL-MOD as the catalyst

linear to monocyclic as a result of dehydration, which occurs on the Ti active centers. This indicates that the cyclic structure with 10 carbon atoms is more preferred in HAL-MOD pores than the linear one.

During catalytic tests, the following the most favorable temperatures were selected: for MMT 80 °C, for MIR 110 °C, for HAL 90 °C and for HAL-MOD 80 °C.

### The influence of catalyst content on geraniol isomerization

In the next stage, the influence of the catalyst content, ranging from 1.0 wt% to 15.0 wt%, on the course of GA transformation in the presence of MMT, MIR, HAL and HAL-MOD was examined.

When the process is carried out in the presence of MMT, the GA conversion is kept practically at a constant level of about 99–100 mol% in the entire range of the tested catalyst content (Table 6). The highest GA conversion values, about 100 mol%, in the case of MIR were obtained for catalyst contents of 2.5 and 5.0 wt%. As the amount of catalyst increases, the function values drop to about 82 mol%. The highest GA conversion values were obtained for HAL of about 99 mol% using 10.0 wt%. catalyst. In the catalyst content range of 2.5–5.0 wt%, the function remained at the level of approx. 75 mol%, and then after exceeding the catalyst content to 10.0 wt%, its values began to drop to 76 mol% (15.0 wt%). The conversion of geraniol in the case of using the modified halloysite is practically constant and amounts to approximately 98–99 mol% in the entire range of the tested catalyst content.

Figure 9 shows the selectivity values of products formed during the geraniol transformation process in the presence of the described catalysts. In the presence of MMT, the products with the highest selectivity values are formed in the range of low catalyst content. The highest values for all formed compounds were obtained at the catalyst content of 1.0 wt% (LO – approx. 36 mol%, DC approx. 27 mol%, TH approx. 28 mol%). As the amount of catalyst increases, their values decrease (Fig. 9a). Figure 9b shows the courses of product selectivity resulting from the process carried out in the presence of MIR. As can

**Table 6.** The influence of the catalyst content on the GA conversion

| Conversion of GA (mol%) | Catalyst content (wt%) | | | | |
|---|---|---|---|---|---|
| | 1.0 | 2.5 | 5.0 | 7.5 | 10.0 |
| MMT | 84.99 | 99.62 | 99.58 | 83.53 | 81.74 |
| MIR | 99.81 | 99.87 | 99.29 | 99.63 | 99.70 |
| | | | | | |
| Conversion of GA (mol%) | 2.5 | 5.0 | 10.0 | 12.5 | 15.0 |
| HAL | 74.94 | 75.75 | 99.43 | 80.67 | 76.54 |
| HAL-MOD | 97.65 | 97.16 | 99.13 | 99.38 | 99.81 |

be seen, when the process is carried out at a low catalyst concentration, i.e., 1.0 wt%, the selectivity of the products is low. The highest DC selectivity values (approx. 44 mol%) are obtained for the catalyst content of 2.5 wt%, and at higher content, its values slightly decrease. The second formed compound is TH, for which the highest values (selectivity approx. 36 mol%) were obtained at 5.0 wt% of the catalyst content. In the range of higher catalyst contents, small amounts of NE are formed. As the catalyst content – HAL – increases, the amount of products formed increases. Their highest amount can be observed at the catalyst content of 10.0 wt%. At this content, TH is formed with the highest selectivity of 14 mol%, followed by DC 8 mol% and NE and LO with similar values. Once the catalyst content exceeds 10 wt%, a sharp decrease in the values of the above-mentioned products is evident, or even their absence (Fig. 9c). Running the process in the presence of modified halloysite, the highest selectivity is obtained for BP, about 60 mol% at the catalyst content of 5 wt% (Fig. 9d). Below this content, the function values are in the range of about 35–37 mol%, while above this the values of this function drop to about 30 mol%. The selectivity values for conversion to DC and TH decrease over the entire range of contents tested: for DC from 24 mol% (1 wt%) to 2 mol% (10 wt%), for TH from 33 mol% (1 wt%) to 5 mol% (10 wt%). Due to the little-developed specific surface area, it can be assumed that the reaction in the presence of HAL-MOD as the catalyst takes place on its surface. The large accumulation of active centers in the form of Ti can lead to dehydration of geraniol molecules, resulting in compounds containing 10 carbon atoms. The high selectivity of the transformation towards BP may indicate that the formation of the cyclic structure is more favored than the formation of compounds with a linear structure.

The most preferred catalyst content for carrying out the GA transformation process was: 1 wt% for MMT, 10 wt% for MIR and HAL, and 5 wt% for HAL-MOD.

**The influence of reaction time on geraniol isomerization**

The influence of reaction time on the course of GA transformation was investigated in the range from 15 min to 24 hours. The remaining parameters (temperature and reaction time) corresponded to the values previously determined as the most favorable.

Table 7 shows the changes in the GA conversion function. In the case of MMT, the conversion slowly increases from about 80 mol% (15 min) to about 100 mol% (180 min) during short reaction times, and then remains at about the same level. When the process is carried out in the presence of MIR, GA conversion remains high at about 97–100 mol% between 15 and 180 minutes. Beyond this time, its values drop to about 72 mol%. In the case of HAL, conversion values increase until 240 minutes and then remain constant at 100 mol%. The situation is different in the case of HAL-MOD, where the conversion of geraniol remains constant over the entire range of reaction times studied, only at longer reaction times oligomerization and polymerization reactions occur.

The selectivity of the conversion to reaction products for MIR is shown in Figure 10b. It is visible that in the initial times of exactly 60 minutes, no products are formed in the process. Only when the process takes 120 minutes and longer the reaction products appear: two dominant ones (DC, TH) and those produced in small amounts (BP, LO, NE). As the reaction time lengthened, the amounts of fragmentation and cyclization products

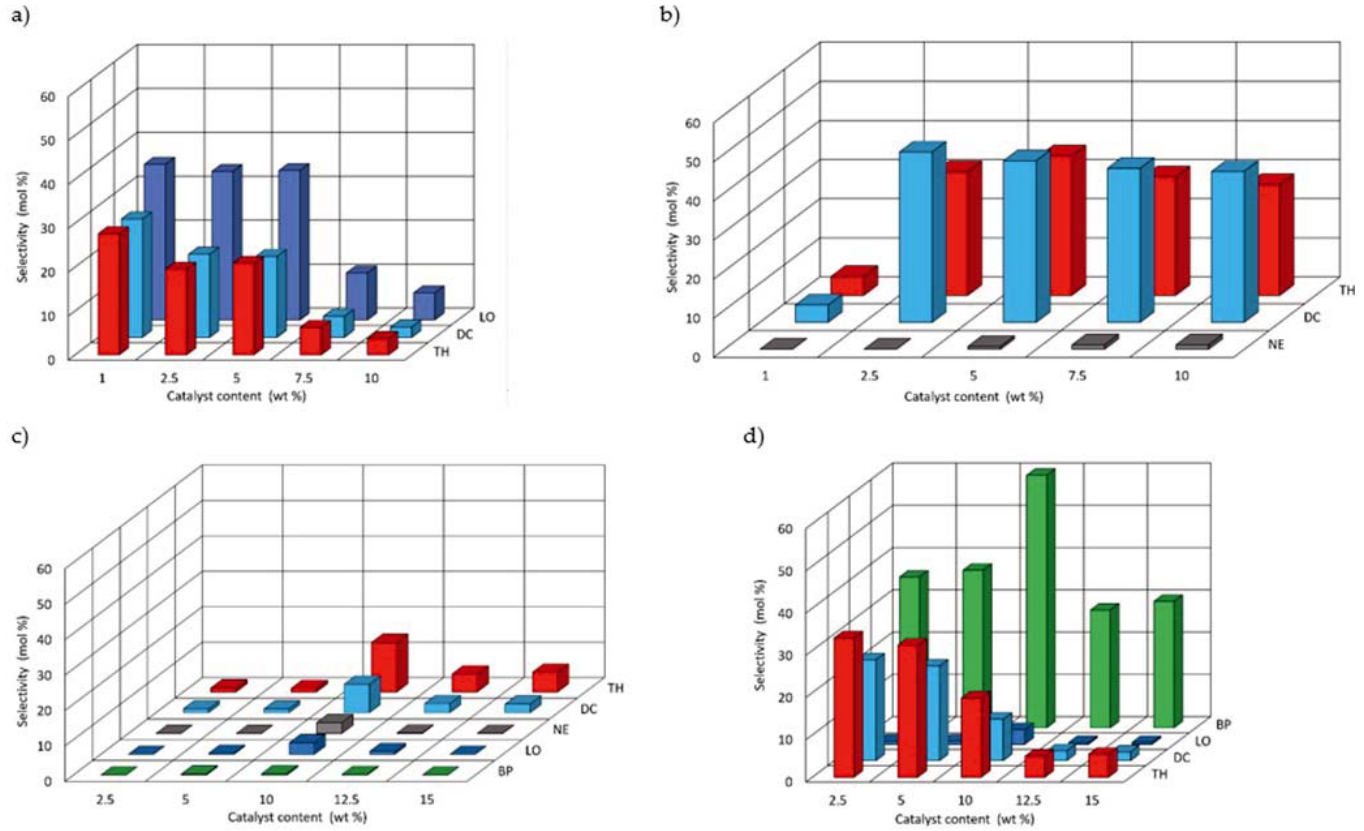


**Figure 9.** The influence of catalyst content on the selectivities of the appropriate products over (a) MMT, (b) MIR, (C) HAL and (d) HAL-MOD as the catalyst

**Table 7.** The influence of the reaction time on the conversion of GA

| Conversion of geraniol (mol%) | Reaction time (min) | | | | | | | | |
|---|---|---|---|---|---|---|---|---|---|
| | 15 | 30 | 60 | 120 | 180 | 240 | 300 | 360 | 1440 |
| MMT | 79.66 | 86.14 | 87.90 | 92.53 | 99.81 | 96.74 | 97.11 | 97.05 | 98.37 |
| MIR | 96.37 | 96.03 | 96.92 | 97.00 | 99.62 | 75.40 | 73.03 | 71.54 | 71.64 |
| HAL | 66.09 | 66.92 | 67.32 | 99.74 | 99.43 | 100.00 | 100.00 | 100.00 | 100.00 |
| HAL-MOD | 99.53 | 99.55 | 99.57 | 99.59 | 99.13 | – | – | – | – |

decreased, and additionally, other reaction products were formed. When the transformation process was carried out in the presence of MMT, three products (LO, DC, TH) were formed. The function flows are similar for all products. In the initial stage, they increase, then reach their maximum, and then decrease. This maximum for most compounds occurs within 120–130 minutes (LO- about 41 mol%, DC – 29 mol%, TH – 29 mol%) (Fig. 10a). In the case of HAL, few products are formed in the short reaction times, while a significant increase can be seen when the reaction takes more than 2 hours. Then the selectivity for TH is about 34 mol%, DC 17 mol%, while other products are produced only in insignificant amounts. Along with the extension of the reaction time, the amounts of the products formed significantly decrease and in the range of 240–1440 min they are practically constant. In the case of HAL-MOD (Fig. 10d), when the process is carried out in a short reaction time of 15 minutes, only BP has formed with a selectivity of approx. 80 mol%. As the reaction time lengthens, other products begin to appear, such as LO, NE, DC and TH, but in much smaller amounts. When the process takes three hours, the selectivity of BP drops while the selectivities of the remaining products are significantly increased. Due to the prolonged reaction time, the analysis of the post-reaction mixture is impossible due to the large amounts of polymerization products produced.

Taking into account the results obtained, the following were chosen as the most favorable reaction times, for the individual catalysts: for MMT, MIR and HAL 120 min, and for HAL-MOD – 15 min.

## CONCLUSIONS

As a result of the research, it turned out that each of the tested minerals MMT, MIR, HAL as well as HAL-MOD are active catalysts in the GA transformation process. Additionally, it can be noticed that each of the tested parameters: temperature, catalyst concentration and reaction time have a significant impact on the GA conversion values and the selectivity of the transformation to individual products. Table 8 shows the most favorable conditions for the GA transformation process.

The study showed that conducting syntheses at higher temperature ranges, with higher catalyst concentrations and using long reaction times resulted in the formation

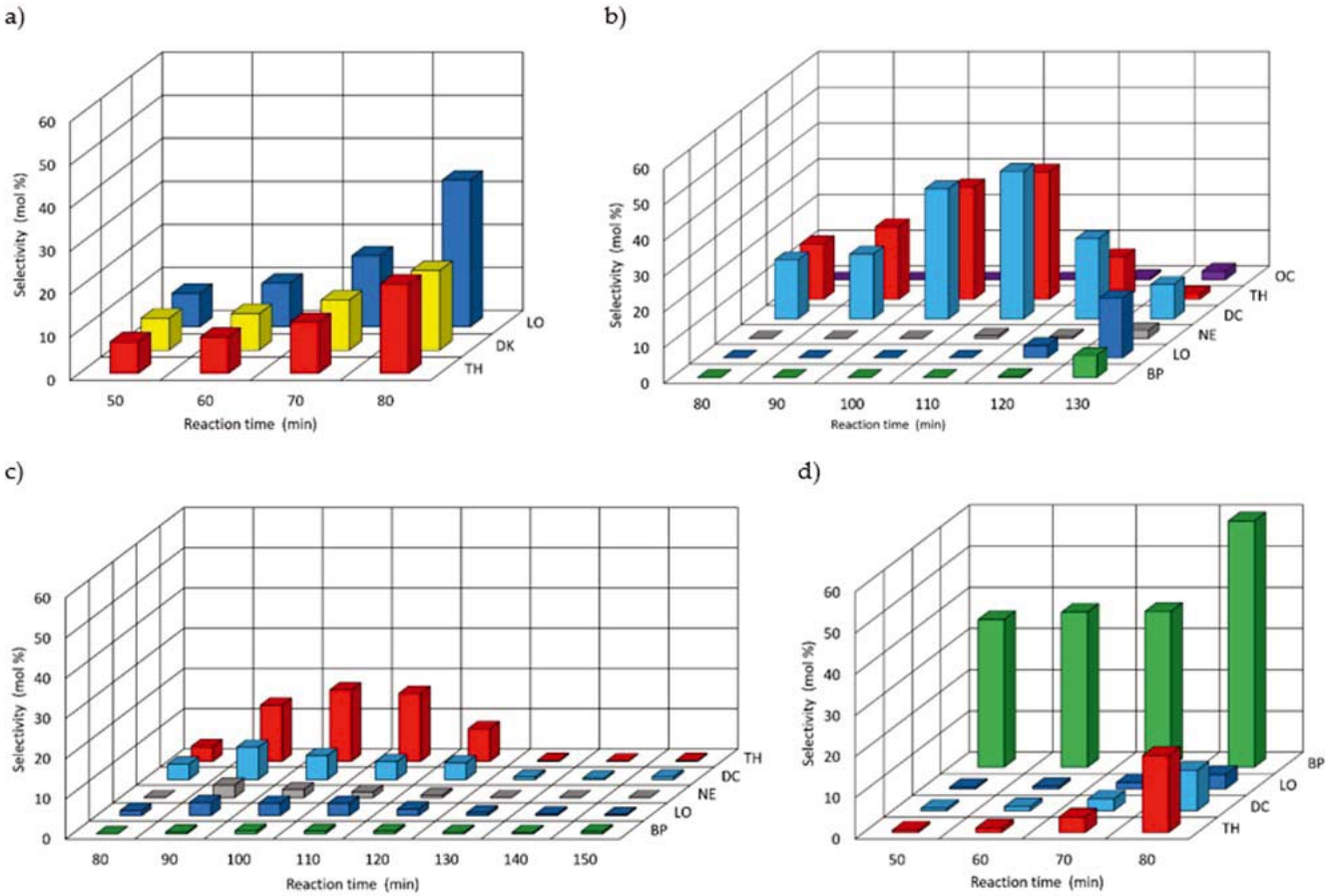


**Figure 10.** The influence of reaction time on the selectivities of the appropriate products over (a) MMT, (b) MIR, (c) HAL and (d) HAL-MOD as the catalyst

**Table 8.** Summary of the most favorable conditions for the GA transformation process for selected catalysts and the obtained conversion selectivity values for individual products

| | MMT | MIR | HAL | HAL-MOD |
|---|---|---|---|---|
| Temperature (°C) | 80 | 110 | 90 | 80 |
| Catalyst content (wt%) | 1 | 10 | 10 | 5 |
| Reaction time (min) | 120 | 120 | 120 | 15 |
| | | | | |
| The obtained selectivity values of the transformation to individual reaction products | $S_{LO}$ = 41.08 mol%<br>$S_{DC}$ = 28.11 mol%<br>$S_{TH}$ = 28.95 mol% | $S_{DC}$ = 47.32 mol%<br>$S_{TH}$ = 36.15 mol% | $S_{DC}$ = 17.10 mol%<br>$S_{TH}$ = 33.87 mol% | $S_{BP}$ = 78.26 mol% |

of polymerization products or products undesirable in the process, which adversely affected the overall analytical performance of the process. Overall, comparing the results for the different catalysts, we found that despite the small BET surface area, HAL-MOD obtained the most favorable (low temperature, catalyst concentration and short time) conditions for the GA transformation process. Equally favorable conditions were obtained for MMT, which may be due to its strongly developed BET surface area and relatively large Vpor. MIR is characterized by a very small BET surface area, while a large Vpor and Vmicrop. which definitely influenced the results obtained. HAL is characterized by a moderately developed BET surface area, as in the case of Vpor and Vmicrop. In conclusion, the conducted research showed that each of the studied parameters significantly affects the results obtained in the transformation of geraniol. Both the structure and morphology of the minerals used have a significant impact on the resulting products. HAL attenuation with hydrochloric acid undoubtedly influenced the results obtained. Due to the undeveloped specific surface area, it can be assumed that the reaction in the presence of HAL-MOD as a catalyst takes place on its surface. A large accumulation of Ti active centers can lead to dehydration of geraniol molecules, resulting in compounds containing 10 carbon atoms. In addition, a great advantage of the presented method is the absence of solvent in the reaction medium, the presence of which could cause additional reactions with GA and consequently lead to the formation of more products.

In the future, new research directions on the process of isomerization of geraniol may involve the use of other porous materials of natural origin. Other research directions on this process may include increasing the pressure (pressure process using an autoclave with a Teflon liner) and determining the optimal solvent. Also worth considering is the topic of process optimization using the Responce Surface Methodology (RSM), which could be helpful in providing a more accurate description of this process.

## LITERATURE CITED

1. Perec, A., Radomska-Zalas, A., Fajdek-Bieda, A. (2022). Modeling of High Pressure Abrasive Water Jet Cutting of Marble. *Facta Universitatis, Series: Mech. Engin.*, 20, 145–156, DOI: 10.22190/FUME210203037P.

2. Fajdek-Bieda, A. (2021). Using Entropy-VIKOR Method in Chemical Processes Optimization. *Proc. Comp. Sci.*, 192, 4208–4217, DOI: 10.1016/j.procs.2021.09.197.

3. Moein, M., Zarshenas, M.M. & Delnavaz, S. (2014). Chemical Composition Analysis of Rose Water Samples from Iran. *Pharmac. Biol.*, 52, 1358–1361, DOI: 10.3109/13880209.2014.885062.

4. Fajdek-Bieda, A., Perec, A. & Radomska-Zalas, A. (2021). Orthogonal Array Approach Optimization of Catalytic Systems. *Proc.Comp. Sci.*, 192, 4200–4207, DOI: 10.1016/j.procs.2021.09.196.

5. Hawari, H.F., Samsudin, N.M., Md Shakaff, A.Y., Ghani, Supri. A., Ahmad, M.N., Wahab, Y. & Hashim, U. (2013). Development of Interdigitated Electrode Molecular Imprinted Polymer Sensor for Monitoring Alpha Pinene Emissions from Mango Fruit. *Proc. Engin.*, 53, 197–202, DOI: 10.1016/j.proeng.2013.02.026.

6. Nissen, L., Zatta, A., Stefanini, I., Grandi, S., Sgorbati, B., Biavati, B. & Monti, A. (2010). Characterization and Antimicrobial Activity of Essential Oils of Industrial Hemp Varieties (Cannabis Sativa L.). *Fitoterapia*, 81, 413–419, DOI: 10.1016/j.fitote.2009.11.010.

7. Laird, K., Kurzbach, E., Score, J., Tejpal, J., Chi Tangyie, G. & Phillips, C. (2014). Reduction of Legionella Spp. in Water and in Soil by a Citrus Plant Extract Vapor. *Applied. Environ. Microb.*, 80, 6031–6036, DOI: 10.1128/AEM.01275-14.

8. Russo, E.B. (2011). Taming THC: Potential Cannabis Synergy and Phytocannabinoid-Terpenoid Entourage Effects: Phytocannabinoid-Terpenoid Entourage Effects. *British J. Pharmac.*, 163, 1344–1364, DOI: 10.1111/j.1476-5381.2011.01238.x.

9. Randrianarivelo, R., Sarter, S., Odoux, E., Brat, P., Lebrun, M., Romestand, B., Menut, C., Andrianoelisoa, H., Raherimandimby, M. & Danthu, P. (2009). Composition and Antimicrobial Activity of Essential Oils of Cinnamosma Fragrans. *Food Chemistry*, 114, 680–684, DOI: 10.1016/j.foodchem.2008.10.007.

10. Trytek, M., Paduch, R., Fiedurek, J. & Kandefer-Szerszeń, M. (2007). Monoterpenes – Old Compounds, New Applications and Biotechnological Methods for Their Obtainment. *Biotechnology*, 76, 135–155 (in Polish).

11. Zdrojewicz, Z., Minczakowska, K. & Klepacki, K. (2014). The Role of Aromatherapy in Medicine. *Family Medicine and Primary Care Review*, 16, 387–391.

12. Yu, W., Wen, M., Yang, L. & Liu, Z. (2002). Ferric Chloride Catalyzed Isomerization and Cyclization of Geraniol, Linalool and Nerol. *Chinese Chemical Letters*, 13, 495–496.

13. Haese, F., Ebel, K., Burkart, K., Unverricht, S. & Münster, P. Method for Isomerizing Allyl Alcohols 2006.

14. Srivastava, P., Wagh, R.S. & Naik, D.G. (2010). γ-Irradiation: A Simple Route for Isomerization of Geraniol into Nerol and Linalool. *Radiochemistry*, 52, 561–564, DOI: 10.1134/S1066362210050206.

15. Tsitsishvili, V., Ramishvili, T., Ivanova, I., Dobryakova, I., Bukia, T. & Kokiashvili, N. (2018). Formation of Long-Chain and Macrocyclic Compounds during Catalytic Conversion of Geraniol on Micro-and Micro-Mesoporous BEA-Type Zeolite. *Bulletin of the Georgian National Academy of Sciences*, 12, 62–69.

16. Fajdek-Bieda, A., Wróblewska, A., Miądlicki, P., Szymańska, A., Dzięcioł, M., Booth, A.M. & Michalkiewicz, B. (2020). Influence of Technological Parameters on the Isomerization of Geraniol Using Sepiolite. *Catalysis Letters* , 150, 901–911, DOI: 10.1007/s10562-019-02987-1.

17. Fajdek-Bieda, A., Wróblewska, A., Miądlicki, P., Tołpa, J. & Michalkiewicz, B. (2021). Clinoptilolite as a Natural, Active Zeolite Catalyst for the Chemical Transformations of Geraniol. *Reac. Kin. Mech. Catal.*, 133, 997–1011, DOI: 10.1007/s11144-021-02027-3.

18. Królikowski, W. & Rosłaniec, Z. Polymer Nanocomposites. *Composites* 2004, *R. 4, nr 9*, 3–15 (in Polish).

19. Bolewski, A., Budkiewicz, M. & Wyszomirski, P. *Ceramic Raw Materials,* Geological Publishers: Warsaw, 1991, ISBN 978-83-220-0412-8 (in Polish).

20. Sarbak, Z. *Adsorption and adsorbents: theory and application,* Chemistry, 1st ed., Adam Mickiewicz University: Poznań, 2000, ISBN 978-83-232-1108-2 (in Polish).

21. Costanzo, P.M. (1984). Static and Dynamic Structure of Water in Hydrated Kaolinites. I. The Static Structure. *Clays and Clay Minerals*, 32, 419–428, DOI: 10.1346/CCMN.1984.0320511.

22. Veerabadran, N.G., Price, R.R., Lvov, Y.M. (2007). Clay Nanotubes For Encapsulation And Sustained Release Of Drugs. *NANO*, 02, 115–120, DOI: 10.1142/S1793292007000441.

23. Utracki, L.A. *Clay-Containing Polymeric Nanocomposites*, Rapra Technology Ltd: Shrewsbury, 2004, ISBN 978-1-85957-437-9.

24. Kuczyńska, H., Kamińska-Tarnawska, E. & Sołtys, J. (2011). Mineral from the "Dunino" Deposits as a Nanosurface for Obtaining Paints. *Chem. Ind. 90*, 138–147 (in Polish).

25. Joussein, E., Petit, S. & Delvaux, B. (2007). Behavior of Halloysite Clay under Formamide Treatment. *Appl. Clay Sci.*, 35, 17–24, DOI: 10.1016/j.clay.2006.07.002.

26. Opaliński, S., Korczyński, M., Kołacz, R., Dobrzański, Z. & Żmuda, K. (2009). Use of Selected Aluminosilicates as Ammonia Adsorbents. *Chem. Industry*, 88, 5, 540–543 (in Polish).

27. Szczygielska, A. & Kijeński, J. (2010). Application of Haloysite as a Filler for Modification of Polypropylene. Part II. Studies of the Properties of the Obtained PP Composites with HNT. *Composites*, *R.,*2, 186–191 (in Polish).

28. Szczygielska, A., Kijeński, J. & Kozłowski, P. *Polymer Modification. Status and Prospects in the Year 2009* (in Polish).

29. Zou, M., Du, M., Zhu, H., Xu, C. & Fu, Y. (2012). Green Synthesis of Halloysite Nanotubes Supported Ag Nanoparticles for Photocatalytic Decomposition of Methylene Blue. *J. Phys.D: Appl. Phys.*, 45, 325302, DOI: 10.1088/0022-3727/45/32/325302.

30. Kamble, R., Ghag, M., Gaikawad, S. & Panda, B.K. (2012). Halloysite Nanotubes and Applications: A Review. *J. Adv. Sci. Res.* 3, 25–29.

31. Lvov, Y. & Abdullayev, E. (2013). Functional Polymer–Clay Nanotube Composites with Sustained Release of Chemical Agents. *Progress in Pol. Sci.*, 38, 1690–1719, DOI: 10.1016/j.progpolymsci.2013.05.009.

32. Jinhua, W., Xiang, Z., Bing, Z., Yafei, Z., Rui, Z., Jindun, L. & Rongfeng, C. (2010). Rapid Adsorption of Cr (VI) on Modified Halloysite Nanotubes. *Desalination*, 259, 22–28, DOI: 10.1016/j.desal.2010.04.046.

33. Barrientos-Ramírez, S., Oca-Ramírez, G.M., Ramos-Fernández, E.V., Sepúlveda-Escribano, A., Pastor-Blas, M.M. & González-Montiel, A. (2021). Surface Modification of Natural Halloysite Clay Nanotubes with Aminosilanes. Application as Catalyst Supports in the Atom Transfer Radical Polymerization of Methyl Methacrylate. *Appl. Catal. A: Gen.*, 406, 22–33, DOI: 10.1016/j.apcata.2011.08.003.

34. Zhang, J., Zhang, D., Zhang, A., Jia, Z. & Jia, D. (2013). Dendritic Polyamidoamine-Grafted Halloysite Nanotubes for Fabricating Toughened Epoxy Composites. *Irian Pol. J.*, 22, 501–510, DOI: 10.1007/s13726-013-0151-5.

35. Bergaya, F. & Lagaly, G. (2006). Chapter 1 General Introduction: Clays, Clay Minerals, and Clay Science. In *Developments in Clay Science*, Elsevier, 1, 1–18, ISBN 978-0-08-044183-2.

36. Masters, A.F. & Maschmeyer, T. (2011). Zeolites – From Curiosity to Cornerstone. *Micropor. Mesopor. Mater.*, 142, 423–438, DOI: 10.1016/j.micromeso.2010.12.026.

37. Armbruster, T. (1993). Dehydration Mechanism of Clinoptilolite and Heulandite: Single-Crystal X-Ray Study of Na-Pooro Ca-, K-, Mg-Rich Clinoptilolite at 100 K. *American Mineralogist*, 78, 260–264.

38. Handke, M. *Crystal chemistry of silicates*, AGH Uczelniane Wydawnictwa Naukowo-Techniczne: Kraków, 2005, ISBN 978-83-7464-016-9 (in Polish).

39. Szymańska, A. Increasing Microporosity of Mironecuton for $CO_2$ Adsorption Process. In Advances in Chemical Technology and Engineering 2018, ZUT Szczecin, Polish Chemical Society: Szczecin, 2018 (in Polish).

40. Kiari, M., Berenguer, R., Montilla, F. & Morallón, E. (2020). Preparation and Characterization of Montmorillonite/PEDOT-PSS and Diatomite/PEDOT-PSS Hybrid Materials. Study of Electrochemical Properties in Acid Medium. *J. Compos. Sci.*, 4, 51, DOI: 10.3390/jcs4020051.

41. Paciorek-Sadowska, J., Borowicz, M., Czupryński, B., Liszkowska, J., & Tomaszewska, E. (2021). Ap plication of halloysite as filler in the production of rigid PUR-PIR foams. *Polimery*, 63(3), 185–190. DOI: 10.14314/polimery.2018.3.3 (in Polish).

42. Machnicka, A. & Nowicka, E. (2016). The use of halloysite to reduce pollutions concentration in municipal wastewater. *Ecol. Engin. & Environ. Technol*., (50), 217–222. DOI: 10.12912/23920629/66853.

43. Kumar Dutta, D., Jyoti Borah, B., & Pollov Sarmah, P. (2015). Recent Advances in Metal Nanoparticles Stabilization into Nanopores of Montmorillonite and Their Catalytic Applications for Fine Chemicals Synthesis. *Catal. Rev.,* 57(3)*,* 257–305*.* DOI: 10.1080/01614940.2014.1003504.

44. Lendzion-Bieluń, Z., Moszyński, D. *Advances in Chemical Technology and Engineering 2018,* ZUT Szczecin, Polish Chemical Society: Szczecin, 2018, ISBN 978-83-7663-266-7 (in Polish).

45. Pajdak, A., Skoczylas, N., Szymanek, A., Lutyński, M. & Sakiewicz, P. (2020). Sorption of $CO_2$ and $CH_4$ on Raw and Calcined Halloysite—Structural and Pore Characterization Study. *Materials*, 13, 917, DOI: 10.3390/ma13040917.

46. Szczepanik, B., Słomkiewicz, P., Garnuszek, M., Rogala, P., Banaś, D., Kubala-Kukuś, A. & Stabrawa, I. (2017). Effect of Temperature on Halloysite Acid Treatment for Efficient Chloroaniline Removal from Aqueous Solutions. *Clay and Clays Minerals***,** 65, 155–167, DOI: 10.1346/CCMN.2017.064056.

47. Djowe, A.T., Laminsi, S., Njopwouo, D., Acayanka, E. & Gaigneaux, E.M. (2013). Surface Modification of Smectite Clay Induced by Non-Thermal Gliding Arc Plasma at Atmospheric Pressure. *Plasma Chemistry and Plasma Processing*, 33, 707–723, DOI: 10.1007/s11090-013-9454-8.

48. Borralleras, P., Segura, I., Aranda, M.A.G. & Aguado, A. (2019). Influence of Experimental Procedure on D-Spacing Measurement by XRD of Montmorillonite Clay Pastes Containing PCE-Based Superplasticizer. *Cement and Concrete Research*, 116, 266–272, DOI: 10.1016/j.cemconres.2018.11.015.

49. Kaufhold, S., Dohrmann, R., Ufer, K. & Meyer, F.M. (2002). Comparison of Methods for the Quantification of Montmorillonite in Bentonites. *Appl. Clay Sci.*, 22, 145–151, DOI: 10.1016/S0169-1317(02)00131-X.

50. Milagres, J.L., Bellato, C.R., Vieira, R.S., Ferreira, S.O. & Reis, C. (2017). Preparation and Evaluation of the Ca-Al Layered Double Hydroxide for Removal of Copper(II), Nickel(II), Zinc(II), Chromium(VI) and Phosphate from Aqueous Solutions. *J. Environ. Chem. Engin.*, 5, 5469–5480, DOI: 10.1016/j.jece.2017.10.013.

51. Wu, X., Liu, C., Qi, H., Zhang, X., Dai, J., Zhang, Q., Zhang, L., Wu, Y. & Peng, X. (2016). Synthesis and Adsorption Properties of Halloysite/Carbon Nanocomposites and Halloysite-Derived Carbon Nanotubes. *Appl. Clay Sci.*, 119, 284–293, DOI: 10.1016/j.clay.2015.10.029.

52. Abdullayev, E., Price, R., Shchukin, D. & Lvov, Y. (2009). Halloysite Tubes as Nanocontainers for Anticorrosion Coating

with Benzotriazole. *ACS Appl. Mater. Interf.*, 1, 1437–1443, DOI:10.1021/am9002028.

53. Bodeepong, S., Bhongsuwan, D., Bhongsuwan, T., Pungrassami, T. (2011). Characterization of Halloysite from Thung Yai Distric, Nackon Si Thammarat Province, in Shouthern Thailand. *J. Sci. and Technol.*, 33, 599–607.

54. Zhang, A.-B., Pan, L., Zhang, H.-Y., Liu, S.-T., Ye, Y., Xia, M.-S. & Chen, X.-G. (2012). Effects of Acid Treatment on the Physico-Chemical and Pore Characteristics of Halloysite. *Coll. Surf. A: Physicochem. Engin. Aspects*, 396, 182–188, DOI: 10.1016/j.colsurfa.2011.12.067.

55. Akpomie, K.G. & Dawodu, F.A. (2016). Acid-Modified Montmorillonite for Sorption of Heavy Metals from Automobile Effluent. *Beni-Suef University J. Basic and Appl. Sci.*, 5, 1–12, DOI: 10.1016/j.bjbas.2016.01.003.

56. Szczepanik, B., Słomkiewicz, P., Garnuszek, M., Czech, K., Banaś, D., Kubala-Kukuś, A. & Stabrawa, I. (2015). The Effect of Chemical Modification on the Physico-Chemical Characteristics of Halloysite: FTIR, XRF, and XRD Studies. *J. Molec. Struc.*, 1084, 16–22, DOI:10.1016/j.molstruc.2014.12.008.